Available online at www.sciencedirect.com
ScienceDirect
Trans. Nonferrous Met. Soc. China 33(2023) 3560−3569
Transactions of Nonferrous Metals Society of China
www.tnmsc.cn

Influence of sulfate ion on fluoride removal from flue gas scrubbing wastewater using lanthanum salts

Xiao-cong ZHONG[1,2,3], Chen CHEN[1], Kang YAN[1,2], Kui-fang ZHANG[1,4], Rui-xiang WANG[1,3], Zhi-feng XU[2]

1. Faculty of Materials Metallurgy and Chemistry, Jiangxi University of Science and Technology, Ganzhou 341000, China;
2. Key Laboratory of Ionic Rare Earth Resources and Environment, Ministry of Natural Resources, Ganzhou 341000, China;
3. Ganzhou Engineering Technology Research Center of Green Metallurgy and Process Intensification, Ganzhou 341000, China;
4. Institute of Resources Utilization and Rare Earth Development, Guangdong Academy of Sciences, Guangzhou 510650, China

Received 17 June 2022; accepted 20 September 2022

Abstract: Batch experiments were conducted to remove fluoride from simulated flue-gas scrubbing wastewater using $La(NO_3)_3·6H_2O$. The effects of SO_4^{2-} concentration and addition sequence on residual fluoride concentration and precipitates properties (mass, morphology, phase structure and composition) were investigated using fluorine ion-selective electrode, SEM, EDS and XRD. The results show that precipitates obtained in the presence of SO_4^{2-} mainly consisted of LaF_3 in irregular bulk shape with high crystallinity. However, amorphous particles were observed in the precipitates, which were speculated to be $La[SO_4]F$. Due to the smaller stoichiometric coefficient of F/La in $La[SO_4]F$ compared to that in LaF_3, the residual fluoride concentration increased as the SO_4^{2-} concentration ascended. Subsequent addition of SO_4^{2-} after lanthanum salt could inhibit the formation of amorphous particles, and further reduce the residual fluoride concentration. At a La/F molar ratio of 1:3.0, the subsequent addition of SO_4^{2-} (0.02 mol/L) after $La(NO_3)_3·6H_2O$ could obtain a residual fluoride concentration of 6.9 mg/L, lower than the required fluoride emission level. Further increasing the La/F molar ratio could reduce residual fluoride concentration to below 2 mg/L, while the risk of retaining La^{3+} would emerge.

Key words: fluoride removal; lanthanum salts; amorphous particles; atomic efficiency; addition sequence

1 Introduction

Excessive intake of fluoride in the long term could lead to dental fluorosis, bone fractures, and skeletal fluorosis [1]. Generally, fluoride in drinking water originates from the geological composition of soils and bedrock [2]. However, semiconductor industry, fluorochemical industry, and metallurgical industry are also significant sources of fluoride emission. Taking metallurgical industry as an example, in the smelting process operated at elevated temperature, fluorine and chlorine in the minerals tend to be volatilized into flue gas in the form of HF and HCl, respectively, which would further merge into the flue gas scrubbing wastewater (FGSW) [3−6]. Along with the recycling of FGSW, the fluoride/chloride concentration of the FGSW gradually ascends to above 300 mg/L, greatly threatening the community water security.

Corresponding author: Rui-xiang WANG, Tel: +86-797-8312204, E-mail: jxustpaper@163.com;
Zhi-feng XU, Tel: +86-797-8312204, E-mail: jxustxzf@163.com
DOI: 10.1016/S1003-6326(23)66354-X

According to a standard (GB 8978—1996) issued by the Ministry of Ecology and Environment of China, the fluorine content in industrial effluent should be less than 10 mg/L. Therefore, the fluoride in FGSW must be removed to the required emission level before discharge.

Several methods are developed to remove fluoride from the groundwater or industrial wastewater, such as chemical precipitation [7−9], adsorption [10−13], coagulation [14], electrodialysis [15], and reverse osmosis [16]. Among these methods, adsorption is most widely reported due to its advantages of large adsorption capacity, low residual fluoride concentration (<1 mg/L), and high availability of adsorbent options [17−20]. However, adsorption method is not cost-effective when treating effluents with high fluoride concentration due to large adsorbent consumption [21]. Hence, in this work, chemical precipitation method is adopted to remove fluoride from FGSW due to its low cost and simple operation.

Conventionally, CaF_2 precipitation is the first choice for fluoride removal from industrial wastewater due to the low cost of precipitation reagent and low solubility product constant (5.3×10^{-9}) of CaF_2. However, CaF_2 precipitation suffers from several problems, such as high final fluoride concentration (10−20 mg/L), sedimentation difficulty caused by fine CaF_2 precipitates, and large amount of wet sludge resulted from $CaSO_4$ [22]. Rare earth fluorides generally own low solubility product constant, especially LaF_3 (7.0×10^{-17}). In addition, $La_2(SO_4)_3$ has a much larger solubility than $CaSO_4$, which could reduce wet sludge production. Therefore, lanthanum salts are more suitable for removing fluoride from FGSW than $CaCl_2$ or lime. In our previous work [23], the chemical behavior of lanthanum and fluorine in simulated FGSW was investigated. The results showed that the distribution of fluoride was significantly determined by the La/F molar ratio. LaF_3 precipitate could be formed only at La/F molar ratio ≤1:3.1. Otherwise, fluoride remained in the solution in the form of LaF_x^{3-x} and cannot be removed from the aqueous solution.

In our previous work, simulated FGSW was prepared with NaF, NaCl, HNO_3, NaOH, and deionized water, among which HNO_3 and NaOH were used for pH adjustment. None competing anions (NO_3^-, CO_3^{2-}, SO_4^{2-}, PO_4^{3-}) are considered in the simulated FGSW. However, some literature reported that competing anions (NO_3^-, CO_3^{2-}, SO_4^{2-}, PO_4^{3-}) could exert adverse effects on the fluoride removal efficiency of La-loaded adsorbents [24−27]. Hence, the effects of anions on the fluoride removal process using lanthanum salt should be clarified. Generally, sulfate ion is the most common anion in FGSW due to the presence of SO_2 in the flue gas. Consequently, the effect of sulfate ion on the variation of solution pH and pF ($-\log(a_{F^-})$), precipitate mass, residual fluoride concentration, precipitate morphology, and precipitate composition were systematically investigated. It was observed that, in the presence of SO_4^{2-}, an amorphous phase was formed in the precipitates during fluoride removal from FGSW using lanthanum salts. Based on the SEM, EDS, XRD and batch experiment results, the generation route of the amorphous phase, and its effects on the fluoride removal process were discussed.

2 Experimental

2.1 Reagents

Synthetic solution was used to stimulate the FGSW. Specifically, synthetic solution was prepared with NaF, NaCl, Na_2SO_4 and deionized water. The fluoride and chloride concentration of the synthetic solution was set as 300 and 1200 mg/L, respectively. Sulfate ion was added in the form of Na_2SO_4. The initial pH of the synthetic solution was adjusted to 5.0 using HNO_3 or NaOH before each batch experiment. In this work, $La(NO_3)_3\cdot6H_2O$ was used as the precipitant. All reagents mentioned above were in chemically pure grade, purchased from Sinopharm®, and used without further purification.

2.2 Experimental procedure and characterization

Batch experiments were conducted to remove fluoride from synthetic solution using $La(NO_3)_3\cdot6H_2O$. Typically, 200 mL of synthetic solution was added in a 250 mL beaker, then $La(NO_3)_3\cdot6H_2O$ was added into the synthetic solution targeting a specific La/F molar ratio. The precipitation reaction was carried out under electromagnetic stirring at 300 r/min and 30 ℃ for 30 min. A fluoride ion-selective electrode and a pH meter were used to monitor the pF and pH of the solution during the precipitation reaction. It is

noteworthy that pF was measured in real-time without pH adjustment. After the precipitation experiment (30 min), the solution was vacuum-filtrated to collect the precipitates. The pF of the filtrate was measured after adjusting the filtrate pH to 5.5, and it was used to calculate the residual fluoride concentration of the filtrate. The precipitates collected were washed with water three times, dried at 80 °C overnight and weighed using electronic balance. Furthermore, the morphology, chemical composition, and phase structure of the precipitates were analyzed using scanning electronic microscopy (SEM), energy dispersive spectroscopy (EDS), and X-ray diffractometer (XRD).

In order to clarify the effect of sulfate ion on the chemical behavior of La^{3+} and F^-, the pF/pH variation, residual fluoride concentration, precipitate mass, precipitate morphology and phase structure were investigated during fluoride removal process with different sulfate ion concentration and SO_4^{2-} addition sequence. In batch experiments with SO_4^{2-} addition after lanthanum salts, lanthanum salts were added into the sulfate-free synthetic solution and reacted for 30 min. Afterwards, SO_4^{2-} was added in the form of Na_2SO_4, and the reaction continued for another 30 min.

3 Results and discussion

Figure S1 (Supplemental Information, SI) shows the digital photos of sulfate- free synthetic solutions after 30 min of precipitation reaction at different La/F molar ratios. It can be found that La/F molar ratio has a significant effect on the fluoride removal process. At a La/F molar ratio lower than 1:3.0 (Figs. S1(a, b)), after 30 min of reaction, the solution became turbid, and a large number of suspended particles appeared. However, at a La/F ratio ≥ 1:3.0 (Figs. S1(c−e)), the solution remained transparent after 30 min of reaction. Namely, adding a theoretical amount or excessive lanthanum salts fails to obtain precipitates. This result was reported in our previous work, which could be explained by the following facts. In aqueous solution with La/F molar ratio ≥ 1:3.0, La^{3+} and F^- tend to form complexes (LaF_x^{3-x}), such as LaF^{2+} and LaF_2^+ ions. In the case of insufficient La^{3+} in the solution (La/F molar ratio < 1:3.0), LaF_x^{3-x} could transfer to LaF_3 precipitate. Therefore, in a sulfate-free synthetic solution, fluoride removal could be achieved only at a La/F molar ratio lower than 1:3.0. However, due to the insufficiency of La^{3+} in the aqueous system, the residual fluoride concentration would surpass the required emission level.

Interestingly, in the synthetic solutions containing 0.02 mol/L SO_4^{2-} (Fig. S2 in SI), regardless of the La/F molar ratio, the synthetic solutions became turbid, and precipitates were observed after 30 min of reaction. Namely, in the presence of sulfate ion, adding excessive or insufficient lanthanum salts could remove fluoride in the form of precipitates. This result signifies that sulfate ion has a significant effect on the chemical behavior of La^{3+} and F^-.

3.1 Fluoride removal from synthetic solution at different La/F molar ratios

Figure 1 shows the variation of pH and pF of the synthetic solution (containing 0.02 mol/L SO_4^{2-}) as a function of reaction time. As shown in Fig. 1(a), upon the addition of lanthanum salt, the pH of the solution dropped sharply and leveled off after 100 s. As the La/F molar ratio increases, the stable pH of the solution decreases correspondingly. Similarly, the pF value of the solution also changed rapidly at the beginning and reached a stable value in 100 s (Fig. 1(b)). Increasing the La/F molar ratio results in a greater stable pF value and lower residual fluoride concentration. These results can be explained by following facts. As a weak acid, the ionization of HF is reversible and keeps in an equilibrium state in the solution (Eq. (1)). Upon the addition of lanthanum salt, a large amount of free F^- was bounded with La^{3+} in the form of LaF_3 (Eq. (2)) or complexes (Eqs. (3) and (4)), leading to an immediate drop of free F^- concentration and increasing pF value. The decreasing of free F^- concentration further enhances the ionization of HF, resulting in a larger H^+ activity and decreasing pH value of the solution.

$$HF \leftrightarrow H^+ + F^- \quad (1)$$

$$La^{3+} + 3F^- = LaF_3 \quad (2)$$

$$La^{3+} + F^- = LaF^{2+} \quad (3)$$

$$La^{3+} + 2F^- = LaF_2^+ \quad (4)$$

Figure 2 shows the precipitate mass and residual fluoride concentration of the solution after 30 min of reaction at different La/F molar ratios. Obviously, at each La/F molar ratio investigated,

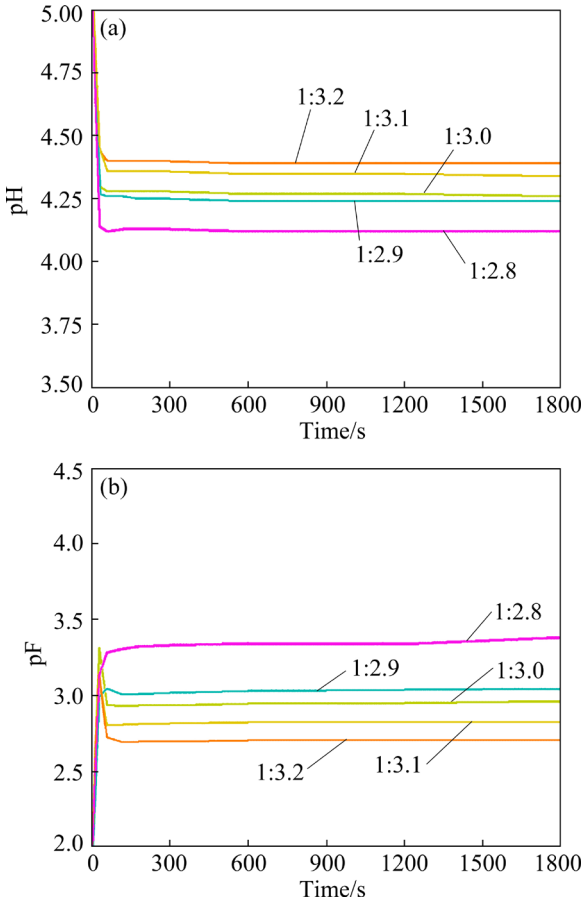

Fig. 1 Variation of pH (a) and pF (b) of synthetic solution (containing 0.02 mol/L SO_4^{2-}) as function of reaction time at different La/F molar ratios (pF measured in real-time without pH adjustment)

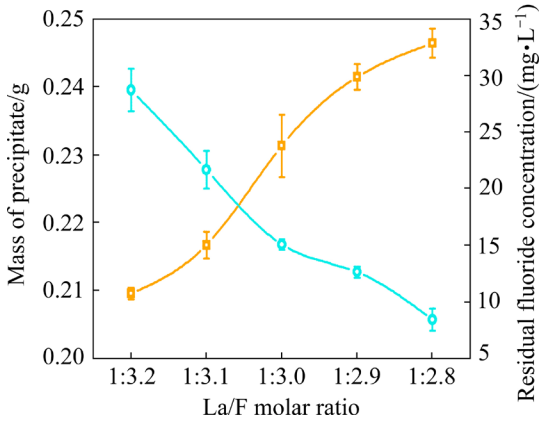

Fig. 2 Precipitate mass and residual fluoride concentration of solution (containing 0.02 mol/L SO_4^{2-}) after 30 min reaction at different La/F molar ratios

precipitates are obtained in the solution, as demonstrated in Fig. S2. As the dosage of lanthanum salt increases, the mass of precipitates obtained increases. Accordingly, the residual fluoride concentration decreases significantly. At the La/F ratio of 1:2.8, the precipitate mass reaches 0.246 g, and the residual fluorine concentration decreases to 8.4 mg/L.

It is worth noting that, according to the total mass of fluorine (60 mg) in each batch experiment, the theoretical production of LaF_3 should be 0.206 g in the case of 100% removal efficiency. As shown in Fig. 2, in sulfate-containing solution, the mass of precipitates is greater than theoretical production regardless of the La/F molar ratio. Specifically, at the La/F ratio of 1:3.0, about 0.232 g precipitate was obtained, exceeding the theoretical production of LaF_3. Moreover, further increasing the La/F molar ratio (adding excessive lanthanum salt) results in a larger precipitate mass. Therefore, it is reasonable to infer that the precipitate would be more complicate than LaF_3, and sulfate ion might involve in the precipitation reaction.

The phase structure of the precipitates obtained in synthetic solution was analyzed by XRD, as shown in Fig. 3. It can be found that the La/F molar ratio barely shows effects on the phase structure of the precipitates. In synthetic solutions with La/F molar ratios ranging from 1:3.2 to 1:2.8, the main phase of the precipitates is LaF_3 regardless of the La/F molar ratio. Even though it is inferred that sulfate ion would be involved in the precipitation reaction, there is no relative phase observed in the XRD patterns.

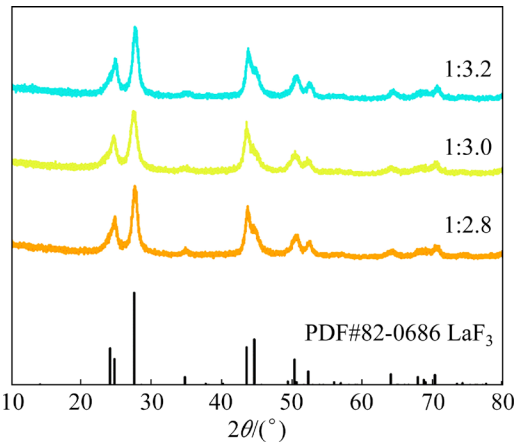

Fig. 3 XRD patterns of precipitates formed in synthetic solutions (containing 0.02 mol/L SO_4^{2-}) at different La/F molar ratios

Figure 4 shows the SEM images of precipitates obtained in synthetic solutions at different La/F molar ratios. It can be found that the precipitates obtained exhibit two structural characteristics: one

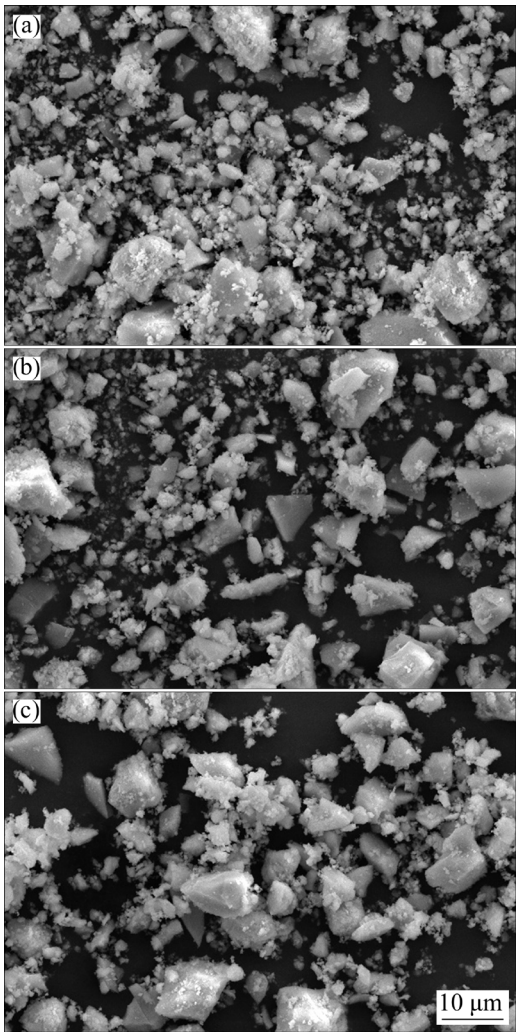

Fig. 4 SEM images of precipitates obtained in synthetic solution (containing 0.02 mol/L SO_4^{2-}) at different La/F ratios: (a) 1:3.2; (b) 1:3.0; (c) 1:2.8

is irregular dense particles with high crystallinity, and the other is loose amorphous particles. This result is also reported in our previous work [23]. According to the XRD results, these dense particles with high crystallinity should be the LaF_3, while the composition of amorphous particles will be discussed below. Comparing the morphologies of precipitates formed at different La/F molar ratios, it can be found that as the La/F ratio increases, the particle size of LaF_3 phase becomes larger, and the amount of amorphous phase seems to increase. This result indicates that excessive lanthanum salts facilitate the formation of amorphous particles.

To elucidate the effect of sulfate ion on the chemical composition of precipitates, the precipitates obtained in synthetic solutions without/with SO_4^{2-} at La/F ratio of 1:3.1 were analyzed by EDS, as shown in Fig. 5. It can be found that in the absence of sulfate ion (Fig. 5(a)), the content of S and O in the precipitate is 0.14 at.% and 0.52 at.%, respectively, which is neglectable. The main elements of the precipitate are La and F, and their contents are 25.8 at.% and 73.5 at.%, respectively. The La/F molar ratio is close to 3:1, confirming the formation of LaF_3. In the presence of sulfate ion (Fig. 5(b)), the content of S and O in the precipitates is 2.90 at.% and 11.72 at.%, respectively. Obviously, the S/O molar ratio is close to 4:1, signifying the presence of SO_4^{2-} in the participates, which proves the analysis of the data shown in Fig. 2. Despite the existence of SO_4^{2-} in the precipitate, the mass fraction of SO_4^{2-} is only 6.37 wt.%, denoting that the main component of the precipitates is still LaF_3, which is in accordance with the XRD results.

3.2 Effect of sulfate concentration on fluoride removal from synthetic solution

To evaluate the influence of sulfate ion on the fluoride removal process, the precipitate mass and residual fluoride concentration in synthetic solutions with different SO_4^{2-} concentrations were measured, as shown in Fig. 6. It is apparent that precipitate mass increases as the SO_4^{2-} concentration ascends, signifying that SO_4^{2-} facilitates the formation of precipitates. Given that the precipitates are LaF_3, as the precipitates mass increases, the residual fluoride concentration is supposed to descend. However, as shown in Fig. 6, the residual fluoride concentration of the solution ascends as SO_4^{2-} concentration increases. Therefore, the increasing precipitate mass could be attributed to the incorporation of SO_4^{2-} in the precipitates, which is in accordance with the analysis mentioned above.

Considering the absence of characteristic peaks of other phase except LaF_3 and the presence of SO_4^{2-} in the precipitates, it is reasonable to infer that SO_4^{2-} might be involved in the formation of amorphous phase. Since $La[CO_3]F$ is the main mineral of bastnasite [28], it is speculated that La^{3+} may combine with SO_4^{2-} and F^- to form $La[SO_4]F$, which has similar structure with $La[CO_3]F$. Due to the amorphous structure of $La[SO_4]F$ in the precipitates, there is no apparent characteristic peak in XRD pattern which could be assigned to $La[SO_4]F$. Since $La[SO_4]F$ has a larger molar mass

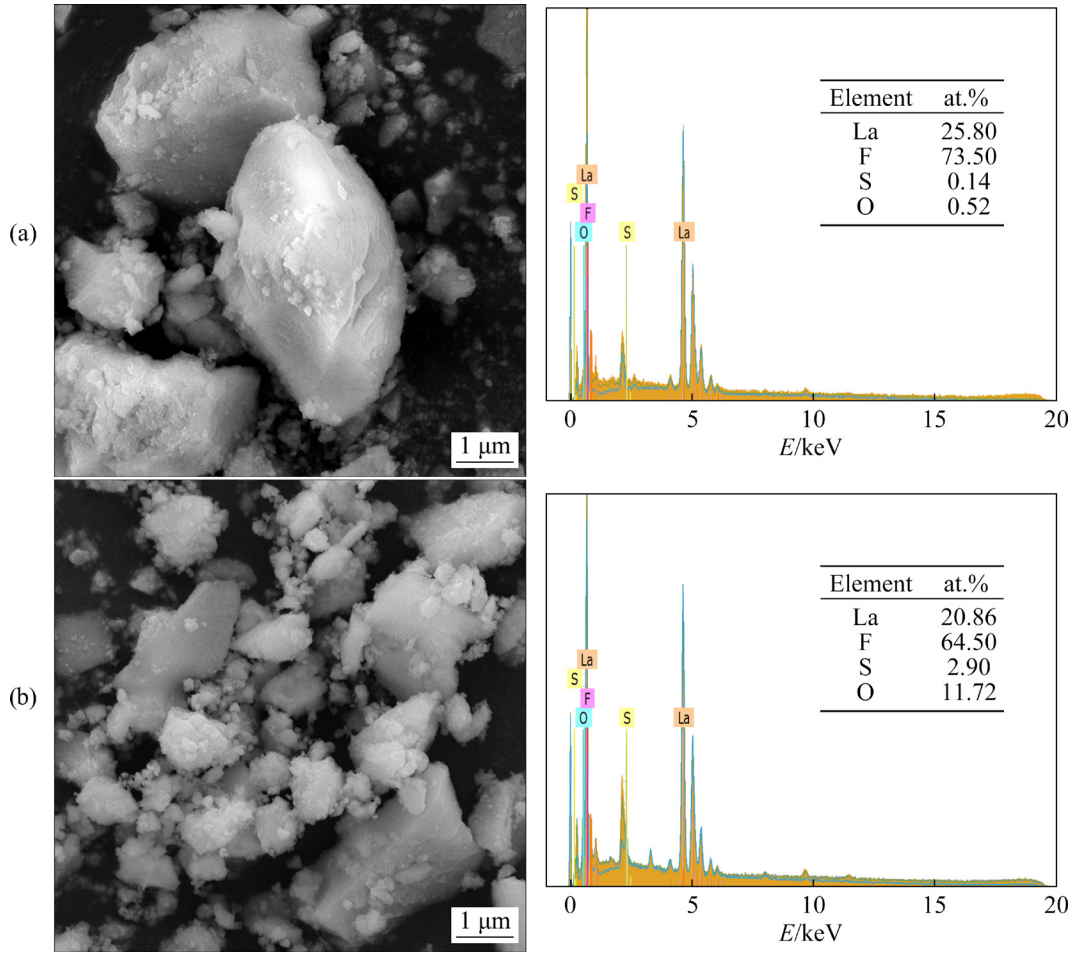

Fig. 5 EDS spectra and elemental composition of precipitates obtained in synthetic solution without (a) or with (b) sulfate ions at La/F molar ratio of 1:3.1

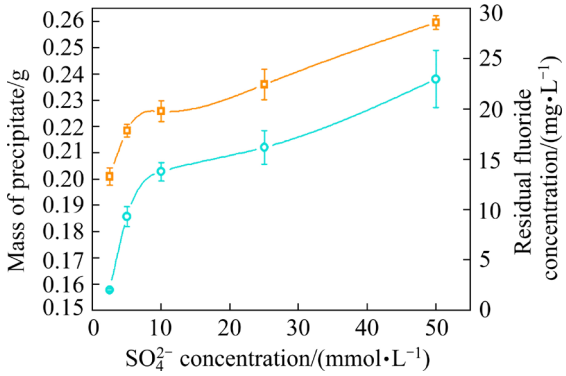

Fig. 6 Effect of SO_4^{2-} concentration on precipitate mass and residual fluoride concentration of solutions after 30 min reaction at La/F ratio of 1:3.0

than LaF_3, the precipitates show greater mass than the theoretical production of LaF_3. Additionally, the stoichiometric coefficient of F/La in La[SO_4]F is 1, smaller than that in LaF_3. Hence, the formation of La[SO_4]F would reduce the atomic efficiency of La^{3+} for fluoride removal. This could explain the increasing residual fluoride concentration in synthetic solution as SO_4^{2-} concentration ascends. In summary, the presence of SO_4^{2-} in FGSW would lead to the formation of amorphous La[SO_4]F, and further reduce the fluoride removal efficiency. Therefore, when treating FGSW with high SO_4 concentration, the dosage of lanthanum salt should be increased slightly.

Figure 7 shows the XRD patterns of the precipitates obtained in synthetic solutions with different SO_4^{2-} concentrations. It can be found that in the absence of SO_4^{2-}, the characteristic peak of LaF_3 located at 28° exhibits the largest intensity and smallest half-height width. As the SO_4^{2-} concentration increases, the characteristic peak at 28° presents a smaller intensity and bigger half-height width, signifying that the increasing SO_4^{2-} concentration leads to lower crystallinity of the precipitates. This result could be attributed to the larger proportion of amorphous La[SO_4]F in precipitates obtained in synthetic solution with increasing SO_4^{2-} concentration.

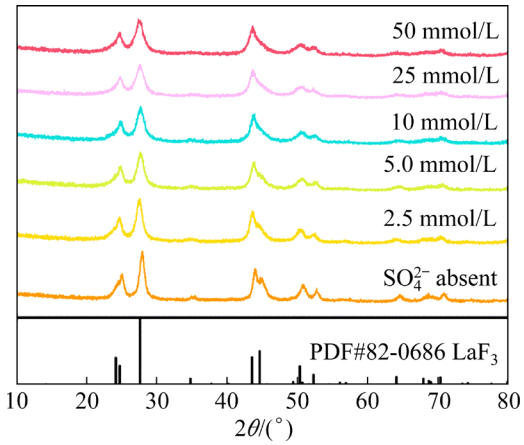

Fig. 7 XRD patterns of precipitates obtained in synthetic solutions with different SO_4^{2-} concentrations after 30 min reaction at La/F ratio of 1: 3.1

3.3 Effect of sulfate addition sequence on fluoride removal from synthetic solution

To uncover the role of SO_4^{2-} in the precipitation reaction, solution pH/pF variation, precipitate mass, residual fluorine concentration and precipitate morphology were investigated with different SO_4^{2-} addition sequence. In these batch experiments, $La(NO_3)_3·6H_2O$ was added to the sulfate-free synthetic solution at the beginning, while SO_4^{2-} was added at the 30th min. Figure 8 shows the variation of solution pH and pF as a function of time before and after the addition of SO_4^{2-}. Before the addition of SO_4^{2-} (in the first 30 min), the fluoride in the solution mainly exists in the form of LaF_3 or LaF_x^{3-x}, which depends on the La/F molar ratio. As shown in Fig. 8, upon the addition of SO_4^{2-}, the solution pH ascends sharply, and the pF drops substantially. At the end of the test, regardless of the La/F ratio, the addition of SO_4^{2-} results in a larger stable pH and a lower stable pF value compared with those before SO_4^{2-} addition. This result could be explained as follows. Upon the addition of SO_4^{2-}, free F^-, La^{3+}, and SO_4^{2-} in the solution could react and form $La[SO_4]F$ via Eq. (5). In addition, the LaF_x^{3-x} or even LaF_3 in the solution formed before SO_4^{2-} addition could also transfer into $La[SO_4]F$ through Eqs. (6)−(8). As Eqs. (6)−(8) show, the formation of $La[SO_4]F$ is accompanied with release of free fluoride. Consequently, the addition of SO_4^{2-} contributes to the increase of free fluoride concentration in the solution, which could explain the descending pF value. The increasing free fluoride concentration further facilitates the association of H^+ and F^-, leading to the decrease of H^+ activity and increase of solution pH.

$$La^{3+}+F^-+SO_4^{2-}=La[SO_4]F \quad (5)$$

$$LaF_2^+ +SO_4^{2-}=La[SO_4]F+F^- \quad (6)$$

$$LaF^{2+}+SO_4^{2-}=La[SO_4]F \quad (7)$$

$$LaF_3+SO_4^{2-}=La[SO_4]F+2F^- \quad (8)$$

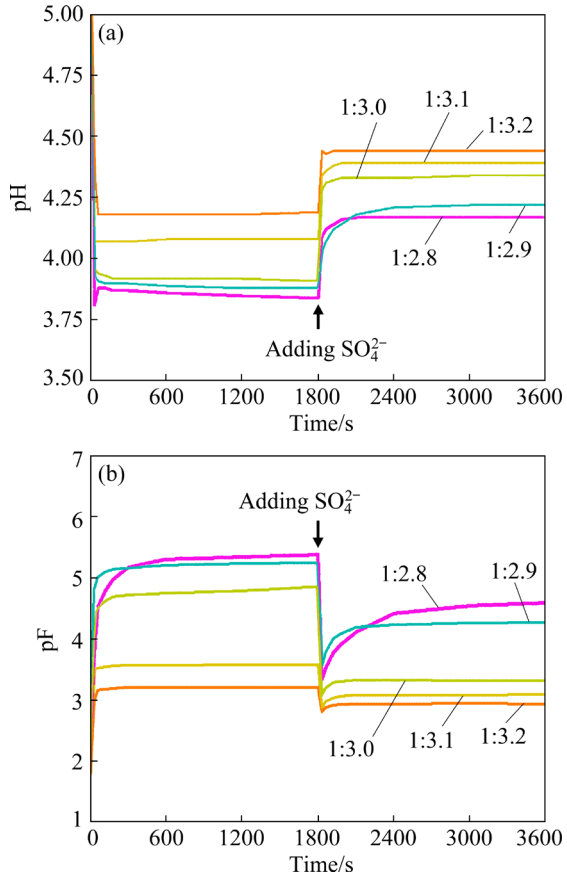

Fig. 8 Variation of pH (a) and pF (b) of solution as function of reaction time (SO_4^{2-} was added in form of Na_2SO_4 at 30 min)

Figure 9 shows the precipitate mass and residual fluoride concentration in synthetic solutions after 60 min reaction (SO_4^{2-} added at the 30th min) at different La/F molar ratios. Comparing the data shown Figs. 2 and 9, it can be found that the addition sequence of SO_4^{2-} and La^{3+} exerts slight effect on the precipitate mass. However, the subsequent addition of SO_4^{2-} is beneficial to reduce the residual fluoride concentration, regardless of the La/F molar ratio. Specifically, at a La/F ratio of 1:3.0, the residual fluoride concentration in batch experiment with subsequent addition of SO_4^{2-} is about 6.9 mg/L, while as 15.1 mg/L fluoride retaining in synthetic solution which contains SO_4^{2-}

initially (adding SO_4^{2-} before La^{3+}). In the case of subsequent addition of SO_4^{2-}, further increasing the La/F molar ratio (≥1:2.9), a lower residual fluoride concentration (<2 mg/L) could be obtained, while the risk of retaining La^{3+} would emerge.

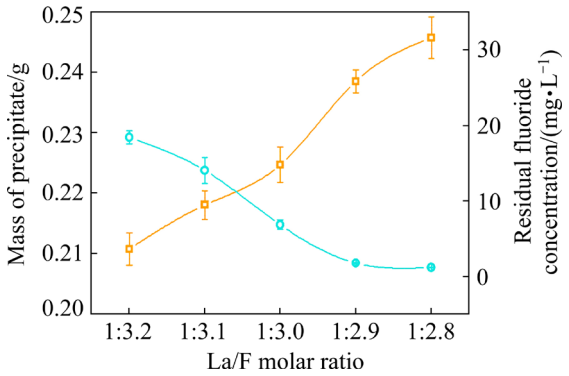

Fig. 9 Precipitates mass and residual fluoride concentration in synthetic solutions after 60 min reaction (SO_4^{2-} was added in form of Na_2SO_4 at 30 min)

To clarify the relationship between addition sequence of SO_4^{2-}/La^{3+} with residual fluoride concentration, the morphologies of precipitates formed in different addition sequence of SO_4^{2-}/La^{3+} have been observed and compared. Figure 10 shows the morphologies of precipitates obtained in batch experiments at different La/F ratios, during which $La(NO_3)_3·6H_2O$ was added at the beginning, while SO_4^{2-} was added at the 30 min. Comparing the morphologies of precipitates shown in Figs. 6 and 10, it is apparent that regardless of La/F molar ratio, subsequent addition of SO_4^{2-} after lanthanum salt facilitates the formation of LaF_3 with high crystallinity, while as substantially reduces the content of amorphous phase in the precipitate. Namely, in the case of subsequent adding SO_4^{2-} after lanthanum salt, the precipitates contain a larger proportion of LaF_3 and less $La[SO_4]F$, which improves the atomic efficiency of La^{3+} and contributes to lower residual fluoride concentration, as demonstrated in Fig. 9. The effect of addition sequence of La^{3+}/SO_4^{2-} on the content of amorphous $La[SO_4]F$ in the precipitate would be explained by the different kinetics of two $La[SO_4]F$ generation routes. In synthetic solution containing SO_4^{2-} originally, upon the addition of La^{3+}, the $La[SO_4]F$ could quickly formed through homogenous reaction via Eq. (5), resulting in precipitates with a larger amount of amorphous $La[SO_4]F$. However, in synthetic solution without SO_4^{2-}, upon the addition of La^{3+}, LaF_x^{3-x} or LaF_3 formed in solution at the beginning. Upon the subsequent addition of SO_4^{2-}, due to the limited free F^- in the solution, $La[SO_4]F$ could only be generated through the transfer of LaF_x^{3-x} or LaF_3 (Eqs. (6)−(8)). Due to much slower kinetics of transferring of LaF_x^{3-x} or LaF_3 comparing with the homogenous reaction route (Eq. (5)), only a small part of LaF_x^{3-x} or LaF_3 could transfer into $La[SO_4]F$. Consequently, the precipitates obtained in the case of adding SO_4^{2-} after lanthanum salt presents much lower content of the amorphous $La[SO_4]F$.

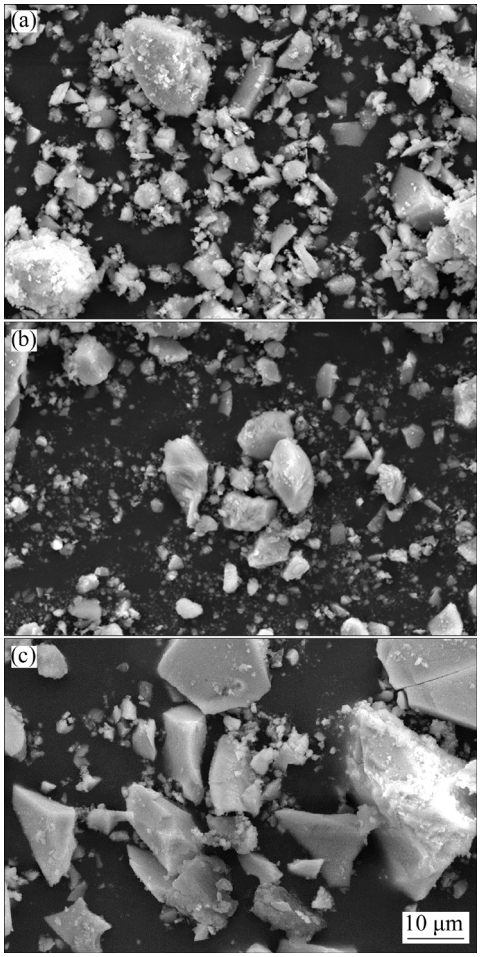

Fig. 10 SEM images of precipitates obtained in synthetic solution after 60 min reaction at different La/F ratios: (a) 1:3.2; (b) 1:3.0; (c) 1:2.8 (SO_4^{2-} was added in form of Na_2SO_4 at 30 min)

4 Conclusions

(1) In simulated flue gas scrubbing wastewater with sulfate ions, regardless of the La/F molar ratio, fluoride could be removed in the form of precipitates. The precipitates obtained in sulfate-containing solution consist of LaF_3 with high

crystallinity and amorphous particles, and the latter was speculated to be La[SO_4]F.

(2) The formation of amorphous La[SO_4]F reduces the atomic efficiency of La^{3+}, which results in ascending residual fluoride concentration as SO_4^{2-} concentration increases.

(3) Subsequent addition of SO_4^{2-} after lanthanum salt could inhibit the formation of amorphous La[SO_4]F in precipitates, which would further improve the atomic efficiency of La^{3+} and reduce the residual fluoride concentration.

(4) The presence of sulfate ion could facilitate the fluoride removal in the form of LaF_3 precipitates even at high La/F molar ratios (≥1:3.0). However, the formation of amorphous La[SO_4]F would reduce the atomic efficiency of La^{3+} and lead to higher residual fluoride concentration. When treating flue gas scrubbing wastewater with high sulfate concentration, the dosage of lanthanum salts should be increased reasonably.

Acknowledgments

This work was financially supported by the National Key Research and Development Program of China (No. 2019YFC1908405), Natural Science Foundation of Jiangxi Province, China (No. 20202BAB214015), Training Plan for Academic and Technical Leaders of Major Disciplines in Jiangxi Province, China (No. 20212BCJ23006), Program of Qingjiang Excellent Young Talents, Jiangxi University of Science and Technology, China, Guangdong Basic and Applied Basic Research Foundation, China (No. 2021A1515012268), China Postdoctoral Science Foundation (No. 2021M702504), and Distinguished Professor Program of Jinggang Scholars in Institutions of Higher Learning, Jiangxi Province, China.

Supplemental Information

Supplemental Information in this paper can be found at: http://tnmsc.csu.edu.cn/download/25-p3560-2022-0677-Supplementary_Information.pdf.

References

[1] DÍAZ-FLORES P E, ARCIBAR-OROZCO J A, FLORES-ROJAS A I, RANGEL-MÉNDEZ J R. Synthesis of a chitosan–zeolite composite modified with La(III): Characterization and its application in the removal of fluoride from aqueous systems [J]. Water, Air, & Soil Pollution, 2021, 232(6): 235.

[2] CHAE G T, YUN S T, MAYER B, KIM K H, KIM S Y, KWON, J S, KIM K, KOH Y K. Fluorine geochemistry in bedrock groundwater of South Korea [J]. Science of the Total Environment, 2007, 385(1/2/3): 272−283.

[3] ÇINARŞAHIN Ç, DERIN B, YÜCEL O. Chloride removal from zinc ash [J]. Scandinavian Journal of Metallurgy, 2000, 29(5): 224−230.

[4] KAHVECIOGLU Ö, DERIN B, YÜCEL O. Carbothermal recovery of zinc from brass ash [J]. Mineral Processing and Extractive Metallurgy, 2003, 112(2): 95−101.

[5] MARTINS J M, DUTRA A J B, MANSUR M B, GUIMARÃES A S. Comparison of oxidative roasting and alkaline leaching for removing chloride and fluoride from brass ashes [J]. Hydrometallurgy, 2021, 202: 105619.

[6] LAI Y Q, YANG K, YANG C, TIAN Z L, GUO W C, LI J. Thermodynamics and kinetics of fluoride removal from simulated zinc sulfate solution by La(III)-modified zeolite [J]. Transactions of Nonferrous Metals Society of China, 2018, 28(4): 783−793.

[7] TURNER B D, BINNING P, STIPP S L S. Fluoride removal by calcite: Evidence for fluorite precipitation and surface adsorption [J]. Environmental Science and Technology, 2005, 39(24): 9561−9568.

[8] CHANG M F, LIU J C. Precipitation removal of fluoride from semiconductor wastewater [J]. Journal of Environmental Engineering, 2007, 133(4): 419−425.

[9] HUANG H M, LIU J H, ZHANG P, ZHANG D D, GAO F M. Investigation on the simultaneous removal of fluoride, ammonia nitrogen and phosphate from semiconductor wastewater using chemical precipitation [J]. Chemical Engineering Journal, 2017, 307: 696−706.

[10] YANG K, LI Y F, TIAN Z L, PENG K, LAI Y Q. Removal of fluoride ions from $ZnSO_4$ electrolyte by amorphous porous Al_2O_3 microfiber clusters: Adsorption performance and mechanism [J]. Hydrometallurgy, 2020, 197: 105455.

[11] RAVURU S S, JANA A, DE S. Performance modeling of layered double hydroxide incorporated mixed matrix beads for fluoride removal from contaminated groundwater with the scale up study [J]. Separation and Purification Technology, 2021, 277: 119631.

[12] SADHU M, BHATTACHARYA P, VITHANAGE M, SUDHAKAR P P. Adsorptive removal of fluoride using biochar—A potential application in drinking water treatment [J]. Separation and Purification Technology, 2021, 278(3): 119106.

[13] HUANG L, YANG Z H, YAN L J, ALHASSAN S I, GANG H Y, WANG T, WANG H Y. Preparation of 2D carbon ribbon/Al_2O_3 and nitrogen-doped carbon ribbon/Al_2O_3 by using MOFs as precursors for removing high-fluoride water [J]. Transactions of Nonferrous Metals Society of China, 2021, 31(7): 2174−2188.

[14] SANDOVAL M A, FUENTES R, NAVA J L, COREÑO O, LI Y M, HERNÁNDEZ J H. Simultaneous removal of fluoride and arsenic from groundwater by electrocoagulation using a filter-press flow reactor with a three-cell stack [J]. Separation and Purification Technology, 2019, 208: 208−216.

[15] BELKADA F D, KITOUS O, DROUICHE N, AOUDJ S, BOUCHELAGHEM O, ABDI N, GRIB H, MAMERI N.

Electrodialysis for fluoride and nitrate removal from synthesized photovoltaic industry wastewater [J]. Separation and Purification Technology, 2018, 204: 108−115.
[16] SHEN J J, RICHARDS B S, SCHÄFER A I. Renewable energy powered membrane technology: Case study of St. Dorcas borehole in Tanzania demonstrating fluoride removal via nanofiltration/reverse osmosis [J]. Separation and Purification Technology, 2016, 170: 445−452.
[17] MILLAR G J, COUPERTHWAITE S J, WELLNER D B, MACFARLANE D C, DALZELL S A. Removal of fluoride ions from solution by chelating resin with imino-diacetate functionality [J]. Journal of Water Process Engineering, 2017, 20: 113−122.
[18] YAN L, TU H W, CHAN T S, JING C Y. Mechanistic study of simultaneous arsenic and fluoride removal using granular TiO_2-La adsorbent [J]. Chemical Engineering Journal, 2017, 313: 983−992.
[19] WANG J, WU L Y, LI J, TANG D D, ZHANG G K. Simultaneous and efficient removal of fluoride and phosphate by Fe−La composite: Adsorption kinetics and mechanism [J]. Journal of Alloys and Compounds, 2018, 753: 422−432.
[20] HE Y X, ZHANG L M, AN X, WAN G P, ZHU W J, LUO Y M. Enhanced fluoride removal from water by rare earth (La and Ce) modified alumina: Adsorption isotherms, kinetics, thermodynamics and mechanism [J]. Science of the Total Environment, 2019, 688: 184−198.
[21] ZHOU J, ZHU W K, YU J, ZHANG H P, ZHANG Y D, LIN X Y, LUO X G. Highly selective and efficient removal of fluoride from ground water by layered Al−Zr−La Tri-metal hydroxide [J]. Applied Surface Science, 2018, 435: 920−927.
[22] HE J Y, YANG Y, WU Z J, XIE C, ZHANG K S, KONG L T, LIU J H. Review of fluoride removal from water environment by adsorption [J]. Journal of Environmental Chemical Engineering, 2020, 8(6): 104516.
[23] ZHONG X C, CHEN C, YAN K, ZHONG S P, WANG R X, XU Z F. Efficient coagulation removal of fluoride using lanthanum salts: Distribution and chemical behavior of fluorine [J]. Frontiers in Chemistry, 2022, 10: 859969.
[24] ANNOUAR S, MOUFTI A, MOUNTADAR S, MOUNTADAR M, SOUFIANE E A. The influences of the presence of ions counter on the removal capacity fluorides ions by chitosane [J]. Oriental Journal of Chemistry, 2016, 32(1): 399−406.
[25] ARAHMAN N, MULYATI S, LUBIS M R, TAKAGI R, MATSUYAMA H. The removal of fluoride from water based on applied current and membrane types in electrodialysis [J]. Journal of Fluorine Chemistry, 2016, 191: 97−102.
[26] ZHANG J F, BRUTUS T E, CHENG J M, MENG X G. Fluoride removal by Al, Ti and Fe hydroxides and coexisting ion effect [J]. Journal of Environmental Sciences, 2017, 57: 190−195.
[27] KUNDU S, CHOWDHURY I H, SINHA P K, NASKAR M K. Effect of organic acid-modified mesoporous alumina toward fluoride ions removal from water [J]. Journal of Chemical and Engineering Data, 2017, 62(7): 2067−2074.
[28] OWENS C L, NASH G R, HADLER K, FITZPATRICK R S, ANDERSON C G, WALL F. Zeta potentials of the rare earth element fluorcarbonate minerals focusing on bastnäsite and parisite [J]. Advances in Colloid and Interface Science, 2018, 256: 152−162.

SO_4^{2-}对烟气洗涤废水镧盐除氟的影响

钟晓聪[1,2,3]，陈 晨[1]，严 康[1,2]，张魁芳[1,4]，王瑞祥[1,3]，徐志峰[2]

1. 江西理工大学 材料冶金化学学部，赣州 341000；
2. 自然资源部离子型稀土资源与环境重点实验室，赣州 341000；
3. 赣州市绿色冶金与过程强化工程技术研究中心，赣州 341000；
4. 广东省科学院 稀土资源利用与开发研究所，广州 510650

摘 要：以 $La(NO_3)_3·6H_2O$ 为沉淀剂从模拟烟气洗涤废水脱除氟离子。采用氟离子选择性电极、SEM、EDS 和 XRD 研究 SO_4^{2-}浓度和添加顺序对残留氟浓度和沉淀性质(质量、形貌、物相和成分)的影响规律。结果表明，在含 SO_4^{2-}模拟烟气洗涤废水中生成的沉淀主要为不规则块状的 LaF_3 晶体。然而，沉淀中同时存在无定形态颗粒，推断其为 $La[SO_4]F$。与 LaF_3 相比，$La[SO_4]F$ 中 F/La 化学计量系数更小，La 原子利用效率更低。因此，随着模拟烟气洗涤废水 SO_4^{2-}浓度增加，残留氟浓度上升。采用镧盐-SO_4^{2-}的添加顺序可以抑制无定形 $La[SO_4]F$ 的生成，有利于降低残留氟浓度。当 La/F 摩尔比为 1:3.0，依次添加 $La(NO_3)_3·6H_2O$ 和 SO_4^{2-}(0.02 mol/L)，可将模拟烟气洗涤废水氟离子浓度降至 6.9 mg/L，低于排放标准。进一步提高 La/F 摩尔比，可以获得更低的残留氟浓度(< 2 mg/L)，然而可能导致 La^{3+}残留的风险。

关键词：除氟；镧盐；无定形颗粒；原子利用效率；添加顺序

(Edited by Xiang-qun LI)